International Journal of Scientific Research in Engineering and Management (IJSREM)
Volume: 09 Issue: 07 | July - 2025 SJIF Rating: 8.586 ISSN: 2582-3930

Synthesis and Characterization of Samarium-Doped Nickel-Cobalt Ferrite Nanoparticles for Advanced Magnetic Applications

G.Sowmya[1*], D. Ravinder[1*]

[1]Department of Physics, Osmania University, Hyderabad, Telangana-500007, India.

Corresponding Author: ravindergupta28@rediffmail.com, sowmyagaripelli@gmail.com

Abstract:

Nanoparticles of samarium-doped nickel-cobalt ferrites with the formula $Ni_{0.7}Co_{0.3}Fe_{2-x}Sm_xO_4$ (x = 0.00 and 0.015) were successfully synthesized using the citrate gel auto-combustion method. X-ray diffraction analysis confirmed the formation of a pure cubic spinel phase, with a slight reduction in lattice constant from 8.3502 Å to 8.3319 Å as samarium content increased, indicating the substitution of Sm^{3+} ions into the spinel lattice. The crystallite size decreased from approximately 35.2 nm for the undoped sample to 23.5 nm for the doped sample, reflecting the influence of samarium on grain growth. Field Emission Scanning Electron Microscopy revealed spherical particles with some agglomeration, typical of chemically synthesized ferrite nanoparticles. Magnetic studies showed a modest decrease in saturation magnetization from 30.6 emu/g to 29.6 emu/g and remanent magnetization from 16.0 emu/g to 15.2 emu/g upon doping, along with a slight decline in the coercivity ratio, indicating altered magnetic interactions due to Sm^{3+} incorporation. These modifications highlight the potential of samarium-doped Ni-Co ferrite nanoparticles for use in magnetic storage, microwave devices, sensors, and biomedical applications such as drug delivery and magnetic hyperthermia.

Keywords: Samarium-doped ferrites, Ni-Co ferrite nanoparticles, Citrate gel auto-combustion, Nanoparticle morphology.

1. Introduction:

Spinel ferrites, represented by the general formula $MO{\cdot}Fe_2O_3$ (where M = Ni^{2+}, Co^{2+}, Zn^{2+}, etc.), crystallize in a face-centered cubic (FCC) structure where oxygen ions form a close-packed arrangement and metal cations occupy two types of interstitial sites—tetrahedral (A) and octahedral (B). The site occupancy and cation distribution in these spinels significantly influence their magnetic and electrical behaviors and are often described using the formula $(A)[B]O_4$, with parentheses and square brackets indicating the respective A and B site cation positions.

Among the various spinel ferrites, nickel ferrite ($NiFe_2O_4$) is known for its soft magnetic nature, moderate saturation magnetization, and high electrical resistivity. On the other hand, cobalt ferrite ($CoFe_2O_4$) is a hard magnetic material with high coercivity, magnetocrystalline anisotropy, and mechanical strength. The partial substitution of Co^{2+} in $NiFe_2O_4$ leads to the formation of mixed Ni–Co ferrites such as $Ni_{0.7}Co_{0.3}Fe_2O_4$, which exhibit a desirable balance of magnetic softness and coercivity, making them suitable for applications in high-frequency transformers, inductors, electromagnetic shielding, and spintronic devices[1 2].

When scaled to the nanoscale, these ferrites display novel properties due to size effects, surface spin disorder, and quantum confinement. Spin canting, surface anisotropy, and magnetically dead layers become significant, influencing the overall magnetic response. As a result, nanostructured spinel ferrites are widely studied for their potential in biomedical applications (e.g., targeted drug delivery, MRI), microwave absorption, catalysis, and magnetic storage[4 5].

The functional properties of spinel ferrites can be effectively tuned by substituting rare-earth ions (RE^{3+}) at the Fe^{3+} sites. Rare-earth dopants, owing to their large ionic radii and localized 4f electrons, introduce lattice strain and modify the superexchange interactions between A and B site cations. Among them, samarium (Sm^{3+}) is particularly interesting due to its high magnetocrystalline anisotropy and large magnetic moment. The substitution of Fe^{3+} with Sm^{3+} (ionic radius ~0.958 Å) in spinel ferrites not only affects the structural and magnetic parameters but also alters the cation distribution, microstrain, and grain growth behavior. However, the larger ionic size of Sm^{3+} compared to Fe^{3+} often leads to phase

separation or the formation of secondary phases such as $SmFeO_3$, which must be avoided to retain the single-phase spinel structure.

To ensure homogeneous mixing of metal cations and to prevent impurity phase formation, wet chemical synthesis techniques are preferred. In this study, the citrate gel auto-combustion method has been employed. This method offers several advantages: it enables molecular-level mixing of precursors, ensures better stoichiometric control, and leads to phase-pure nanoparticles at relatively lower calcination temperatures. Citric acid acts as both a chelating agent and a fuel, producing a self-propagating exothermic reaction during gel decomposition that yields fine-grained, homogeneous ferrite nanoparticles[6 7].

The present work focuses on the synthesis of Sm^{3+}-doped $Ni_{0.7}Co_{0.3}Fe_{2-x}Sm_xO_4$ (0.00 and 0.015) nanoparticles using the citrate gel auto-combustion method. The primary objective is to investigate the influence of Sm^{3+} substitution on the structural, microstructural, and magnetic properties of Ni–Co spinel ferrites. Structural characterization is conducted using X-ray diffraction (XRD) and Fourier-transform infrared spectroscopy (FTIR), while morphological and compositional analyses are performed using scanning electron microscopy (SEM) and energy-dispersive X-ray spectroscopy (EDX). Magnetic behavior is evaluated through vibrating sample magnetometry (VSM). The results aim to provide a comprehensive understanding of how Sm^{3+} doping alters the intrinsic properties of Ni–Co ferrites and their potential applicability in modern electronic and magnetic devices.

2. Experimental Procedure:

Nanocrystalline Sm^{3+}-substituted Ni–Co spinel ferrite nanoparticles with the general composition $Ni_{0.7}Co_{0.3}Fe_{2-x}Sm_xO_4$ (x = 0.00 and 0.015) were synthesized using the citrate gel auto-combustion method. All precursor chemicals were of analytical grade and obtained from Sigma-Aldrich. The synthesis utilized nickel nitrate hexahydrate [$Ni(NO_3)_2 \cdot 6H_2O$], cobalt nitrate hexahydrate [$Co(NO_3)_2 \cdot 6H_2O$], ferric nitrate nonahydrate [$Fe(NO_3)_3 \cdot 9H_2O$], samarium nitrate hexahydrate [$Sm(NO_3)_3 \cdot 6H_2O$], and citric acid monohydrate [$C_6H_8O_7 \cdot H_2O$] as the fuel and complexing agent.Stoichiometric quantities of the metal nitrates were dissolved in deionized water to form a homogeneous solution. Citric acid was added to the mixed solution in a 1:3 molar ratio (metal nitrates:citric acid), ensuring effective chelation of the metal ions. The pH of the solution was carefully adjusted to ~7 by dropwise addition of aqueous ammonia (NH_4OH) under constant magnetic stirring. The resulting clear solution was then heated and stirred continuously at 80–90 °C for approximately 4 hours, leading to the formation of a viscous gel.Subsequent heating of the gel to ~200 °C triggered a self-sustaining combustion reaction, yielding voluminous black powder. The as-combusted powders were calcined at 500 °C for 4 hours in a muffle furnace to improve phase purity and crystallinity by removing residual organic matter. The final product was finely ground using an agate mortar and stored in airtight containers for further structural, morphological, and magnetic characterization.

3. Characterization:

The crystal structure and phase composition of the synthesized $Ni_{0.7}Co_{0.3}Fe_{2-x}Sm_xO_4$ (x = 0.00 and 0.015) nanoparticles were examined using X-ray diffraction (XRD, PANalyticalX'Pert PRO) operated with Cu-Kα radiation (λ = 1.5406 Å) in the 2θ range of 20°–80°. Crystallite sizes were estimated using the Debye–Scherrer equation based on the full width at half maximum (FWHM) of the most intense diffraction peaks.The surface morphology and particle size distribution were analyzed using a Field Emission Scanning Electron Microscope (FESEM, ZEISS ULTRA Plus). The micrographs were used to investigate surface texture, agglomeration behavior, and morphological consistency with the calculated crystallite sizes.Magnetic properties at room temperature were measured using a Vibrating Sample Magnetometer (VSM, Lakeshore 7404) in the magnetic field range of ±15 kOe. Parameters such as saturation magnetization (Ms), coercivity (Hc), and remanent magnetization (Mr) were extracted from the hysteresis loops to evaluate the influence of Sm^{3+} substitution on magnetic behavior.

4. Results and Discussions:

4.1.XRD Studies

The structural analysis of $Ni_{0.7}Co_{0.3}Fe_{2-x}Sm_xO_4$ samples with varying samarium content (x = 0.00 and 0.02) was performed using X-ray diffraction. The diffraction patterns confirmed the formation of a single-phase cubic spinel structure without any secondary phases. The lattice constant (**a)** was calculated from the peak positions, showing a slight decrease from 8.3502 Å for the undoped sample to 8.3319 Å with 2 % Sm substitution. This reduction in lattice parameter can be attributed to the substitution of Fe^{3+} ions by smaller Sm^{3+} ions, which influences the crystal lattice dimensions.Crystallite sizes were estimated using the Debye–Scherrer formula from the most intense peak, revealing a decrease from approximately 35.2 nm in the pure sample to 23.5 nm for the doped composition[8 9]. This reduction in crystallite size suggests that samarium doping inhibits grain growth during synthesis.The unit cell volume also decreased slightly with Sm doping, from 582.2 $Å^3$ for x = 0.00 to 578.4 $Å^3$ for x = 0.02, consistent with the reduction in lattice constant. These changes indicate successful incorporation of Sm ions into the spinel lattice, affecting both the structural parameters and nanocrystalline nature of the material.

Table 1 summarizes the lattice constants, crystallite sizes, and unit cell volumes for the different compositions.

Table.1 Calculated XRD parameters of Sm^{3+} doped Ni – Co Ferrites.

Composition x	LatticeConstant“a”	Crystallite size(D) nm	Volume(v)
0.000	8.350198	35.21499	582.2242
0.015	8.331892	23.51241	578.4034

Furthermore, the XRD patterns for the samples are shown in **Figure 1**, illustrating the phase purity and peak shifts corresponding to the changes in lattice parameters.

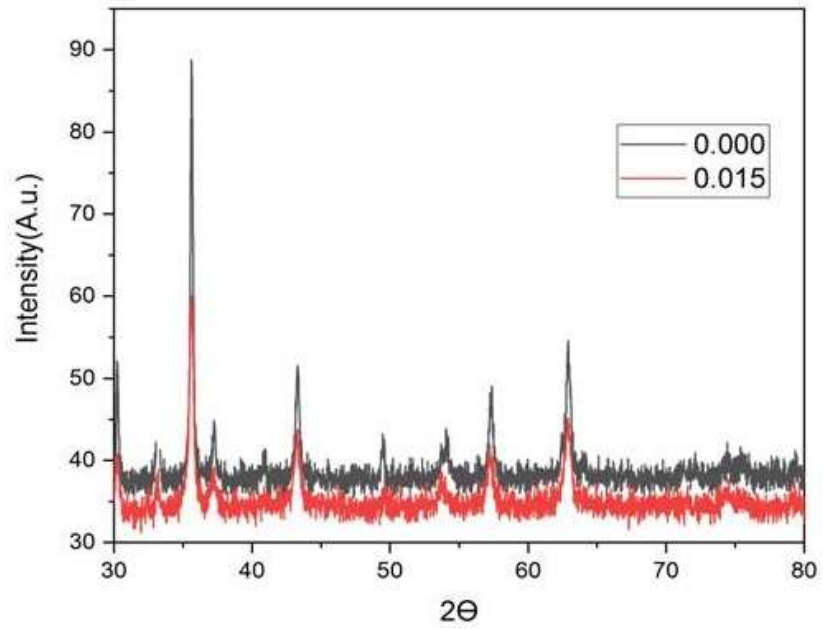

Fig. 1. X- Ray Diffraction patterns of Sm^{3+} doped Ni – Co Ferrites.

4.2 FESEM Studies:

Field Emission Scanning Electron Microscopy (FE-SEM) was utilized to investigate the surface morphology of $Ni_{0.7}Co_{0.3}Fe_{2-x}Sm_xO_4$ samples with x = 0.00 and 0.015. The micrographs reveal that the particles predominantly exhibit a spherical shape with noticeable agglomeration. Such agglomeration is commonly observed in ferrite nanoparticles synthesized via wet chemical methods like citrate gel auto-combustion[10]. The clustering of particles can be primarily attributed to strong magnetic interactions among the nanoparticles, as well as the inherently high surface energy associated with nanoscale materials.

Fig. 2 FE-SEM micrographs of Sm^{3+} doped Ni – Co Ferrites.

4.3 Magnetic Studies:

Magnetic

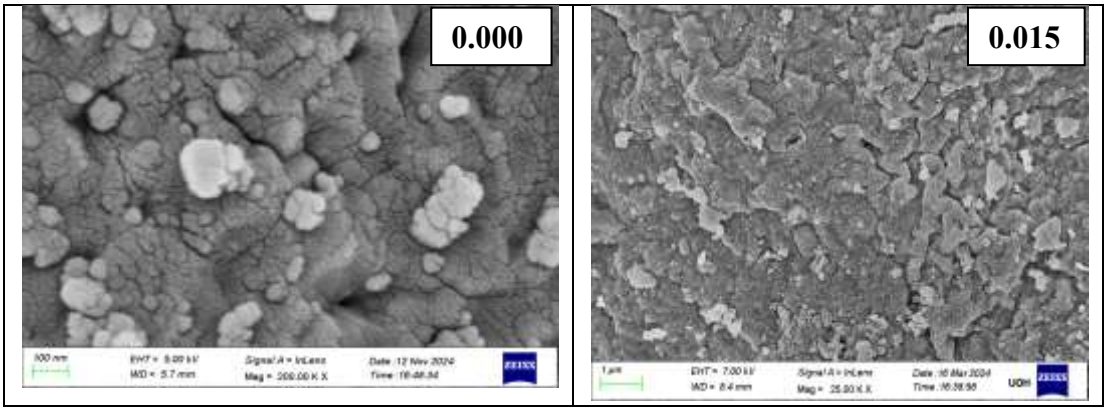

measurements of Sm^{3+} substituted nickel-cobalt ferrite samples were performed using a vibrating sample magnetometer (VSM) coupled with a Physical Property Measurement System (PPMS). This arrangement provided accurate magnetization data as a function of applied magnetic field, enabling thorough assessment of the magnetic response of the synthesized nanoparticles. Key magnetic parameters such as saturation magnetization (M_s), remanent magnetization (M_r), and the remanence ratio (M_r/M_s) were determined from the recorded hysteresis loops.

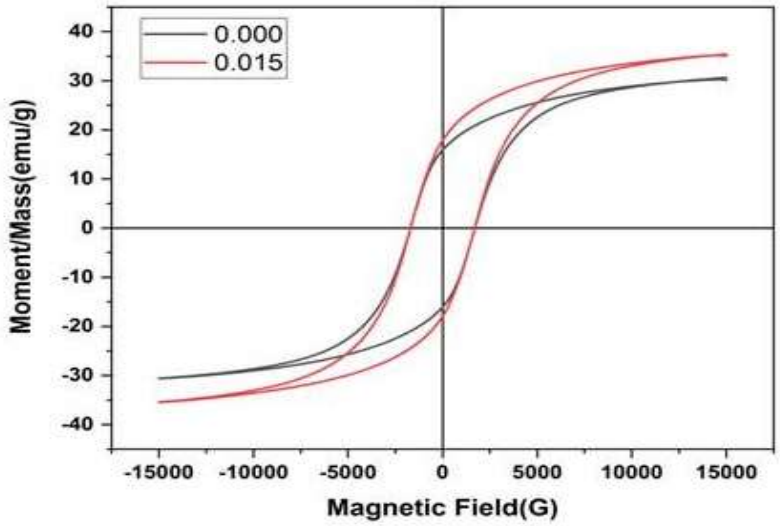

For the undoped sample (x = 0.000), the saturation magnetization was found to be approximately 30.64 emu/g, with a remanent magnetization of 15.98 emu/g and an Mr/Ms ratio close to 0.52. Upon doping with samarium at x = 0.015, a slight decrease in saturation magnetization to 29.59 emu/g and remanent magnetization to 15.20 emu/g was observed,

accompanied by a minor reduction in the Mr/Ms ratio to 0.51[11 12]. This indicates that samarium incorporation induces subtle changes in the magnetic properties, likely due to modifications in the cation distribution and magnetic interactions within the spinel structure.Calculated parameters shown in Table 2.

Table.2 Calculated magnetic parameters of Sm^{3+} doped Ni – Co Ferrites.

Composition x	Ms	Mr	Mr/Ms
0.000	30.63755	15.98347	0.521695
0.015	29.59099	15.19739	0.513581

5.Conclusions:

Samarium-doped $Ni_{0.7}Co_{0.3}Fe_{2-x}Sm_xO_4$ nanoparticles were successfully synthesized using the citrate gel auto-combustion method, resulting in well-defined spinel structures with nanoscale crystallite sizes. The incorporation of Sm^{3+} ions effectively modified the lattice parameters and influenced the magnetic behavior, leading to tunable saturation and remanent magnetization values. The morphological analysis confirmed uniform, mostly spherical nanoparticles with typical agglomeration due to magnetic interactions.These tailored structural and magnetic properties make samarium-doped nickel-cobalt ferrites highly promising for a range of advanced applications. Their adjustable magnetic characteristics and nanoscale dimensions are particularly suited for high-frequency microwave devices, magnetic data storage, sensors, and spintronic technologies. Additionally, their biocompatibility and magnetic response open avenues in biomedical fields such as targeted drug delivery and magnetic hyperthermia treatment.

6. References:

[1].M., I., A., Abdel, Maksoud., Mohamed, Mohamady, Ghobashy., Ahmad, S., Kodous., Ramy, Amer, Fahim., Ahmed, I., Osman., Ala'a, H., Al-Muhtaseb., David, Rooney., Mohamed, A., Mamdouh., Norhan, Nady., A., Ashour. (2022). Insights on magnetic spinel ferrites for targeted drug delivery and hyperthermia applications. Nanotechnology reviews, https://doi.org/10.1515/ntrev-2022-0027.

[2].Muhammad Naeem Kiani, Muhammad Shoaib Butt, Iftikhar Hussain Gul, Mohsin Saleem, Muhammad Irfan, Abrar H. Baluch, Muhammad Aftab Akram, and Mohsin Ali Raza,Synthesis and Characterization of Cobalt-Doped Ferrites for Biomedical Applications, ACS Omega 2023 8 (4), 3755-3761 DOI: https://doi.org/10.1021/acsomega.2c05226

[3].Murotova, Yulduz, Faxriddin, qizi. (2023). Advancements in spinel nanoferrites. https://doi.org/10.1016/b978-0-323-96115-8.00002-7

[4].Bhaskar, Bhaduri., Ashutosh, Dikshit., TaeYoung, Kim., Kumud, Malika, Tripathi. (2022). Research Progress and Prospects of Spinel Ferrite Nanostructures for the Removal of Nitroaromatics from Wastewater. ACS Applied Nano Materials, https://doi.org/10.1021/acsanm.2c02684

[5].Mohan, M., Kumaraswamy. (2023). Ferrite Nanoparticles for Telecommunication Application. Materials horizons, https://doi.org/10.1007/978-981-99-2583-4_6.

[6].Motahareh, Jafarpour., Mohammad, Rostami., S.M.H., Khalkhali., Hossein, Nikmanesh., M.H., Majles, Ara. (2022). The effect of lanthanum substitution on the structural, magnetic, and dielectric properties of nanocrystalline Mn-Ni spinel ferrite for radio frequency (RF) applications. Physics letters, https://doi.org/10.1016/j.physleta.2022.128285

[7].B., B., Raje, Shaikh., Syed, Qadeeruddin, Chishty. (2021). Auto-ignition synthesis of rare-earth metal-doped Ni–Zn spinel ferrites for electronic applications. Journal of Materials Science: Materials in Electronics, https://doi.org/10.1007/S10854-021-06863-W.

[8].Dixit, Aparna & Ahmed, Inas& Abraham, Jisha& El-Bahy, Zeinhom& Manzoor, Mumtaz & Dar, Ahmad & Sharma, Ramesh. (2023). Optoelectronic and thermoelectric properties of spinel chalcogenides HgLa2X4 (X=S and Se): A first-principles study. Journal of Rare Earths. 10.1016/j.jre.2023.11.014. Sweety, Supriya., Sunil, Kumar.,

Manoranjan, Kar. (2017). Band gap engineering of zinc substituted cobalt ferrite for optoelectronic applications. https://doi.org/10.1109/NMDC.2017.8350491

[9].Sweety, Supriya., Sunil, Kumar., Manoranjan, Kar. (2017). Band gap engineering of zinc substituted cobalt ferrite for optoelectronic applications. https://doi.org/10.1109/NMDC.2017.8350491

[10].Yan, Wu., Liang, Liu., Xinxin, Yu., Jing, Zhang., Lingyao, Li., Chunjie, Yan., Bin, Zhu., Bin, Zhu. (2018). Natural hematite ore composited with ZnO nanoneedles for energy applications. Composites Part B-engineering, https://doi.org/10.1016/J.COMPOSITESB.2017.11.020

[11].Haochuan, Wan., Liming, Hu., Xiaohe, Liu., Ying, Zhang., Gen, Chen., Ning, Zhang., Renzhi, Ma. (2023). Advanced hematite nanomaterials for newly emerging applications. Chemical Science, https://doi.org/10.1039/d3sc00180f

[12].Shokrollahi, Hooman. (2017). A review of the magnetic properties, synthesis methods and applications of maghemite. Journal of Magnetism and Magnetic Materials. 426. 74-81. https://doi.org/10.1016/j.jmmm.2016.11.033